sustainability

MDPI

Article

Modeling and Multi-Objective Optimization of NO_x Conversion Efficiency and NH_3 Slip for a Diesel Engine

Bo Liu [1,2], Fuwu Yan [1,2], Jie Hu [1,2,*], Richard Fiifi Turkson [1,2,3] and Feng Lin [1,2]

1 Wuhan University of Technology, Hubei Key Laboratory of Advanced Technology for Automotive Components, Wuhan 430070, China; liubo321@whut.edu.cn (B.L.); yanfuwu@vip.sina.com (F.Y.); rturkson@hopoly.edu.gh (R.F.T.); auto_lf@163.com (F.L.)

2 Hubei Collaborative Innovation Center for Automotive Components Technology, Wuhan 430070, China

3 Mechanical Engineering Department, Ho Polytechnic, P. O. Box HP 217, Ho 036, Ghana

* Correspondence: auto_hj@163.com; Tel.: +86-13071237418

Academic Editor: Marc A. Rosen

Received: 8 April 2016; Accepted: 10 May 2016; Published: 17 May 2016

Abstract: The objective of the study is to present the modeling and multi-objective optimization of NO_x conversion efficiency and NH_3 slip in the Selective Catalytic Reduction (SCR) catalytic converter for a diesel engine. A novel ensemble method based on a support vector machine (SVM) and genetic algorithm (GA) is proposed to establish the models for the prediction of upstream and downstream NO_x emissions and NH_3 slip. The data for modeling were collected from a steady-state diesel engine bench calibration test. After obtaining the two conflicting objective functions concerned in this study, the non-dominated sorting genetic algorithm (NSGA-II) was implemented to solve the multi-objective optimization problem of maximizing NO_x conversion efficiency while minimizing NH_3 slip under certain operating points. The optimized SVM models showed great accuracy for the estimation of actual outputs with the Root Mean Squared Error (RMSE) of upstream and downstream NO_x emissions and NH_3 slip being 44.01×10^{-6}, 21.87×10^{-6} and 2.22×10^{-6}, respectively. The multi-objective optimization and subsequent decisions for optimal performance have also been presented.

Keywords: NO_x conversion efficiency; NH_3 slip; genetic algorithm; support vector machine; prediction model; multi-objective optimization

1. Introduction

Diesel engines are widely used in almost all kinds of commercial vehicles and some passenger vehicles because of their good dynamic performance, fuel economy, and durability. However, one of the main challenges regarding the use of diesel engines is the reduction of NO_x emissions, which is a common air pollutant and may cause photochemical smog. This is especially true against the background that there is a growing global concern over environment pollution and climate change issues resulting from the use of automobiles. Generally, the urea based selective catalytic reduction (urea-SCR) is widely adopted as a promising and efficient technique for decreasing the NO_x emissions [1–4] through redox reactions between NH_3 and NO_x. This technology was first used in stationary applications and has become pretty popular for vehicles over the last decade [5–7].

The main advantages of SCR technology include the fact that it has a high NO_x conversion rate (up to 90% or more) and can improve fuel economy. Furthermore, the reliability and durability of the SCR system are also superb. However, this technique requires external supply of reductant (urea) and will generate additional NH_3 slip because the non-reactive NH_3 will be emitted into the environment.

NH_3 is also a pollutant and may cause severe respiratory diseases. Therefore, the main challenge of the SCR is the control of urea injection amount to deal with the optimal trade-off problem between the NO_x conversion efficiency and NH_3 slip [8].

Researchers have proposed various control strategies and methods for urea injection, including open-loop control [9], closed-loop control [10–12] and model predictive and adaptive control [13–15]. Another way of dealing with this problem is the use of multi-objective genetic algorithms. The first step of the proposed method is to build engine and SCR models for the prediction of the upstream and downstream NO_x emissions and NH_3 slip to obtain the two conflicting objective functions (NO_x conversion efficiency and NH_3 slip) for the multi-objective optimization. The multi-objective optimization method is then used to optimize the decision variable (urea injection amount) to maximize NO_x conversion efficiency while minimizing the NH_3 slip under certain operating points.

Figure 1 shows a schematic of a catalytic converter illustrating how NO_x emissions are converted into nitrogen gas and water. Figure 1 also indicates the possible emissions of non-reactive NH_3 (NH_3 slip) and non-reactive NO_x.

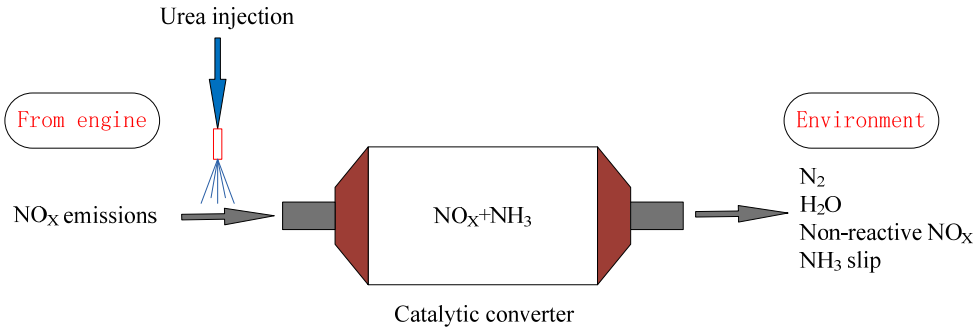

Figure 1. Schematic for the conversion of NO_x to nitrogen and water.

A good number of research activities have been conducted and have proposed a variety of ways for predicting NO_x emissions [16–19]. A study [20] used artificial neural networks to build a prediction model for CO_2, soot, and NO_x. In references [19,21], an adaptive least squares support vector machine model was built for the prediction of NO_x emissions with a novel update to tackle process variations. The support vector machine (SVM), which is established based on the structural risk minimization principle, has proven to exhibit better generalization performance than neural networks and other methods [22]. In the work of Martinez-Moraleset [23], artificial neural networks were used for the non-linear identification of a gasoline engine for the purpose of evaluating objective functions used within an optimization framework involving the use of the NSGA-II genetic algorithm and the Multi-Objective Particle Swarm Optimization (MOPSO) algorithm. It was observed that the NSGA-II algorithm performed better than the MOPSO algorithm in the Pareto based optimization process. In the study [24], it was found, again, that the multi-objective optimization solution for the NSGA-II algorithm was better than that of the ε-constraint method.

Against the background given above, the current study proposed a novel method based on an SVM (Support Vector Machine) and GA (Genetic algorithm) for modeling a target diesel engine and SCR system to predict upstream and downstream NO_x emissions and NH_3 slip. The NSGA-II genetic algorithm was used for the multi-objective optimization involving the maximization of NO_x conversion efficiency while minimizing NH_3 slip because it has proven to give better optimal results compared with other optimization methods as observed in references [23,24].

2. Experimental Setup and Methods

As discussed in Section 1, the first step of the current study is to build prediction models for estimating engine and SCR system output $\hat{y}$ as close as possible to the actual output y for an input

vector $\boldsymbol{X} = (x_1, x_2, x_3, \ldots, x_n)$ using optimal SVM (support vector machine) models. The SVM is the most appropriate method for obtaining the prediction model of a stochastic system from a small amount of experimental data [25]. After obtaining the prediction models, non-dominated sorting genetic algorithm (NSGA-II) was implemented to deal with the trade-off between the two conflicting objective functions of NO_x conversion efficiency and NH_3 slip under certain working points. The whole procedures of modeling and multi-objective optimization were implemented in MATLAB® (MathWorks, Inc., Natick, MA, USA).

2.1. Data Collection

In this study, data was collected by running a four-stroke, six-cylinder YUCHAI YC6L-42 diesel engine on a dynamometer. The main specifications of the experimental engine as well as the dynamometer and associated instrumentation are presented in Tables 1 and 2 respectively. The Eddy-current dynamometer and associated instrumentation were used in the experiments to measure engine speed and torque with the fuel supply per cycle being obtained from the CAN bus directly. The AVL 4000 and the LDS6 instrumentation were used for the measuring of NO_x emissions and NH_3 slip, respectively. In order to cover as many common operating points of the diesel engine as possible, 180 equally spaced operating points were selected, with speed ranging from 900 rpm to 2600 rpm (with a step size of 100 rpm) and engine load ranging from 10% to 100% (with a step size of 10%). Parts of these are shown in Table 3.

Table 1. Technical specifications of the experimental engine.

Features	Parameters
Engine type	YUCHAI YC6L-42
Number of cylinder	6
Displacement volume	6.6 L
Max. power	179 kW
Max. torque	940 N· m
Cooling system	Water-cooled

Table 2. The parameter measurement methods.

Equipment	Measurement Parameters
Eddy current dynamometer	Speed, torque
CAN bus	circulating oil
AVL4000	NO_x emissions
LDS6	NH_3 slip

Table 3. Engine operating conditions.

Mode	Speed (rpm)	Torque (N*m)	Load (%)	Fuel Supply (mg/cyc)	Temperature of Catalyst (°C)	Upstream NO_x (ppm)
1	1000	215	30	171	215	862
2	1000	391	60	309	326	1401
3	1000	585	90	503	492	849
4	1500	204	30	168	250	684
5	1500	408	60	300	344	1131
6	1500	612	90	436	415	1306
7	2000	201	30	178	249	498
8	2000	395	60	299	318	767
9	2000	596	90	429	394	1026
10	2500	153	30	165	227	290
11	2500	312	60	265	296	489
12	2500	471	90	364	378	674

2.2. Data Preprocessing

Generally, there are some numerical discrepancies among input variables x_1, x_2, x_3, ..., x_n, and, as a consequence, some variables may not have a significant influence on the system's output y. Therefore, in order to eliminate the negative impact caused by the huge numerical discrepancies of input variables, there was the need to normalize each variable to vary from 0 to 1. For each column of data sample x_i, the normalized data sample is given by:

$$x_i' = \frac{x_i - x_i\,(min)}{x_i\,(max) - x_i\,(min)} \tag{1}$$

where x_i is the original data, x_i' is the normalized data, and x_i(max) and x_i(min) are the maximum and minimum in x_i, respectively. Subsequently, the normalized data x_i' were used as the inputs for the SVM models.

2.3. Building and Optimizing the SVM Models

The Support Vector Machine (SVM) [26] was developed by Vapnik and Cortes in 1995. As a novel kind of machine learning method, the SVM is gaining increasing popularity because of its many attractive features and promising empirical performance. A detailed description of SVM theory can be found in references [27–29].

Here, only a brief description is given. A support vector machine takes advantage of the kernel function to map the input data onto a high-dimensional feature space. Linear regression is then performed in the high-dimensional feature space. As a result, non-linear problems can be addressed in a linear space through non-linear feature mapping. After training on the input data sample, the SVM model can be used to predict variables whose values are unknown.

The final prediction function used by an SVM is as follows:

$$f(x) = \sum_{i=1}^{m} a_i y_i K(x_i, x) + b \qquad 0 < a_i < C \tag{2}$$

where a_i is Lagrange multiplier, and x_i is a feature vector corresponding to a training variable. The components of vector a_i and the constant b are optimized during training. C is a penalty factor, which indicates the degree of attention paid to outliers and determines the range of a_i. The larger the value of C is the more attention is paid to the outliers. The kernel function is represented by $K\,(x_i, x)$, and is one of the most important parts of the SVM model. There are four common kinds of kernel functions. Among them, the Gaussian radial basis function kernel is most commonly used because of its effectiveness and speed in the modeling process [30].

The Gaussian function takes the form:

$$K(x_i, x) = \exp(-g\ ||x - x_i\ ||^2) \tag{3}$$

where g is the parameter of the kernel function, which is as important as penalty factor C, with x and x_i representing independent variables.

2.4. Model Parameter Optimization with Grid Search and GA

Based on the preceding discussion, it is clear that the kernel function parameters C and g are considerably vital in the SVM model. The selection of parameters C and g directly influences the performance of the SVM model. Thus, it could be deduced that the performance of the SVM model lies in the choice of the kernel function parameter g and penalty factor C. In this study, a multi-algorithm combined method is proposed for optimizing the model parameters.

A Genetic Algorithm (GA) [31] is a kind of optimization algorithm, which uses genetics to simulate the natural evolution process. Three basic operators of selection, crossover and mutation are used to

generate better offspring populations in order to find exact or approximate solutions to optimization problems. GAs have been successfully used to solve a broad spectrum of optimization problems owing to its high effectiveness and lower time consumption [32].

Therefore, in this study, a genetic algorithm was used to optimize the C and g parameters of the SVM model. Furthermore, the k-fold cross-validated root mean squared error (*RMSE*) [33] was selected as the fitness of the objective function for the GA to reflect the prediction accuracy of the SVM model.

$$RMSE = \sqrt{\frac{\sum_{i=1}^{N} (y - \hat{y})^2}{N}} \quad (4)$$

where N is the number of samples, with y and $\hat{y}$ representing the actual and predicted values respectively. The main objective of the GA was to yield the smallest k-fold cross-validated *RMSE* by searching for the best combinations of the C and g parameters for the SVM model.

In a GA, prior to the initial random population generation, the ranges of each parameter need to be given, which are almost given empirically at present. If the ranges were too wide, the optimization process would be time-consuming. On the other hand, if the ranges were too small, the best parameters may not be captured in the ranges. Based on this, a grid search is proposed for determining the rough scope in this study. In addition, existing studies have shown that identifying a good parameter pair by searching exponentially in the sequences is more practical and less time-consuming. For example, $C = 2^{-2}, 2^{-1}, \cdots, 2^{10}$; $g = 2^{-1}, 2^{0}, \cdots, 2^{10}$ [34].

The procedure of optimizing the C and g parameters of the SVM with grid search and GA is shown in Figure 2 as follows:

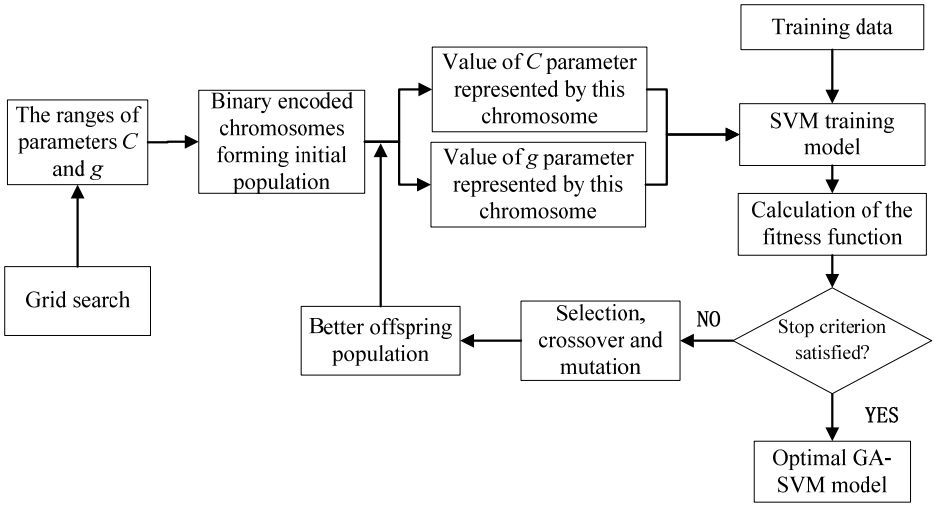

Figure 2. Optimizationn of Support Vector Machine (SVM) model with Genetic Algorithm (GA).

Step 1: Involves the use of a grid search in the range of $C \in [2^{-10}, 2^{15}]$ and $g \in [2^{-5}, 2^{10}]$ according to the exponential sequences mentioned earlier. The k-fold cross-validated *RMSE* for all pairs of C and g parameters is evaluated for the SVM model in the process of finding the best pair.

Step 2: Based on the best pair of C and g parameters determined in Step 1, the ranges of each parameter in the GA are established. Subsequently, a two-dimensional random initial population, which is binary encoded, is created. Each dimension (chromosome) represents C and g, respectively.

Step 3: Involves the calculation of the fitness function of all populations given by the k-fold cross-validated *RMSE* for the SVM model.

Step 4: Based on fitness level (k-fold cross-validated *RMSE*), a better offspring population is generated through the use of the three basic genetic operators of selection, crossover and mutation. In this study, the probabilities for the selection, crossover and mutation operators were set to 0.9, 0.8 and 0.05, respectively.

Step 5: In this step, Step 4 was repeated until the stopping criterion (100 generations for the current study) was satisfied.

After these steps, the best pair of C and g was obtained, ending the optimization process for the SVM models.

2.5. Multi-Objective Optimization

After building and optimizing the three prediction models for the upstream and downstream NO_x emissions as well as NH_3 slip, the ultimate goal of this study was to optimize the urea injection amount to maximize the NO_x conversion efficiency while minimizing the NH_3 slip, a situation that characterizes a typical multi-objective optimization problem.

A multi-objective optimization problem is usually concerned with maximizing or minimizing a number of objective functions in the presence of certain inequality and equality constraints, as well as other constraints in the form of lower and upper bounds defining the decision variable space. Generally, multi-objective optimization problems do not have a single optimal solution but a Pareto optimal set for the conflict between the various goals, and, as a consequence, it is therefore virtually impossible for multiple objectives to simultaneously achieve optimal results.

The NSGA-II genetic algorithm was proposed by Kalyanmoy *et al.* [35] to help reduce the computational complexity based on a certain number of decision variables and a given population of solutions, preserve the elite members of a population of solutions and eliminate the need for a sharing parameter associated with other multi-objective evolutionary algorithms like the Pareto-archived evolutionary strategy (PAES) [36] and the strength-Pareto evolutionary algorithm (SPEA) [37]. NSGA-II takes advantage of the non-dominated sorting and crowding distance so that the algorithm has the capacity to approximate the best Pareto frontier and ensure that the obtained Pareto optimal solution has a good spreading. The specific description of the NSGA-II can be found in references [35,38,39].

The basic procedure for executing NSGA-II for the current multi-objective problem is summarized in Figure 3 and the steps are as follows:

Step 1: Involves fixing the parameters and the range of the decision variable (urea injection amount). In the current study, an initial solutions population of 100 and a maximum number of generations of 200 were used for the multi-objective optimization. The lower and upper bounds for the urea injection amount variable were 0 and 2000 mL/h, respectively.

Step 2: Based on the parameters and ranges determined in Step 1, a random initial population, which is binary encoded, was created.

Step 3: Involves the calculation of the ranks and crowding distance of the population, followed by the application of the tournament selection method for selecting the best solutions in a particular population for creating a mating pool for producing child solutions based on non-dominated sorting.

Step 4: Involves the generation of offspring and parent population through crossover and mutation operators to ensure that the diversity within different generations of solutions is preserved. The best individuals were selected as the new population from the population incorporating offspring and parent population based on non-dominated sorting. In this study, probabilities of 0.9 and 0.1 were used for the crossover and mutation operators for the multi-optimization framework, respectively.

Step 5: In this step, a repetition of Step 3 and Step 4 was carried out until the stopping criterion (200 generations for the current study) was satisfied.

After these steps, the optimal Pareto set of the decision variable (urea injection amount) was obtained.

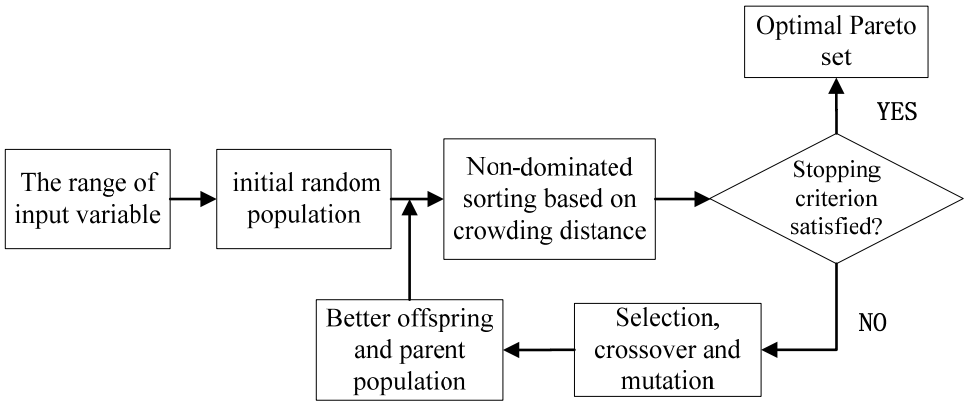

Figure 3. General procedure for executing the Non-dominated Sorting Genetic Algorithm (NSGA-II) multi-objective optimization in the current study.

3. Results and Discussion

3.1. Results for SVM Model Simulation

Based on the modeling and optimization methods discussed in Section 2, three prediction models were obtained. One was an engine model for predicting upstream NO_x emissions. The other two were an SCR model for predicting downstream NO_x emissions and another for NH_3 slip under different operating points. Half (1/2) of the equally spaced data samples were selected as the training dataset for these optimal SVM models. After the models were trained, the rest 1/2 samples were applied to the model to test the generalization ability of the optimal models. The flow chart for designing the optimal SVM models is shown in Figure 4.

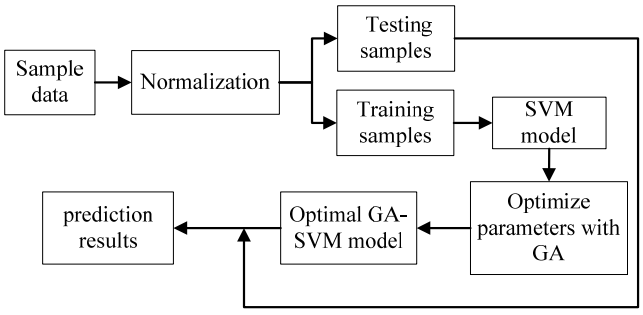

Figure 4. Processes for designing the proposed SVM models.

Figure 5a shows the comparison between the actual outputs and model prediction for the upstream NO_x emissions. Figure 5b also shows the quality of fit between the actual outputs and the model prediction. It is evident from Figure 5a that the curves for actual and predicted values almost coincide, and the errors between them are considerably small. It can also be seen from Figure 5b that all the points are evenly distributed along the line where the predicted values tracked the actual values fairly well, implying that the upstream NO_x emissions were predicted with good accuracy for all samples. Similar statistics are shown graphically for the downstream NO_x emissions and NH_3 slip in Figures 6 and 7 which also show good prediction accuracy.

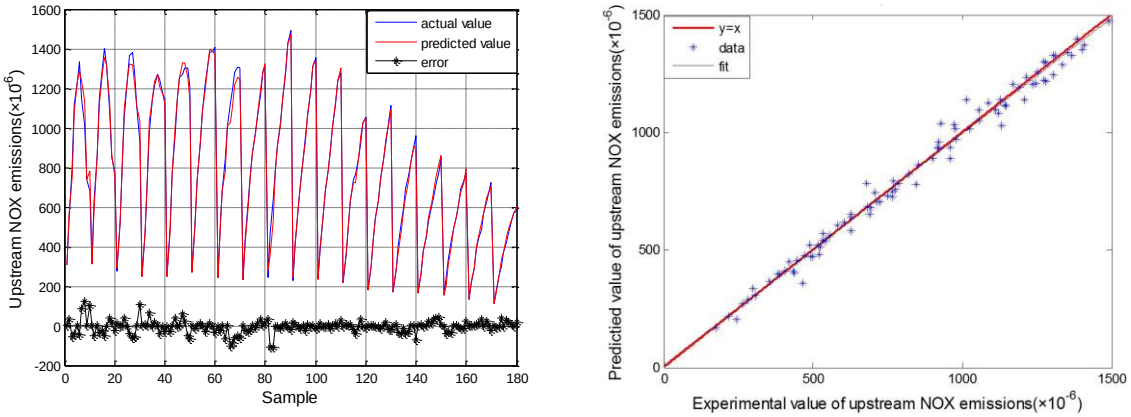

(a) (b)

Figure 5. Comparison between experimental and predicted values for upstream NO_x emissions. (**a**) Actual versus predicted output; (**b**) Quality of fit.

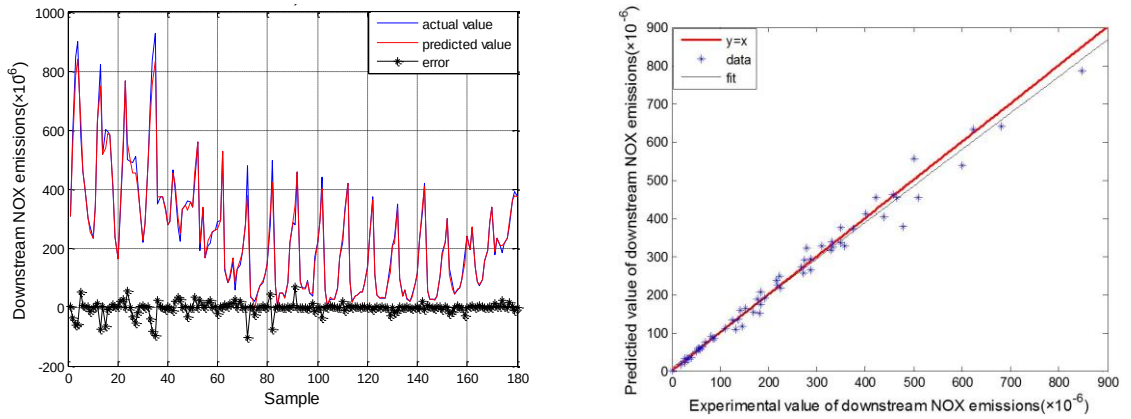

(a) (b)

Figure 6. Comparison between experimental and predicted values for downstream NO_x emissions. (**a**) Actual versus predicted output; (**b**) Quality of fit.

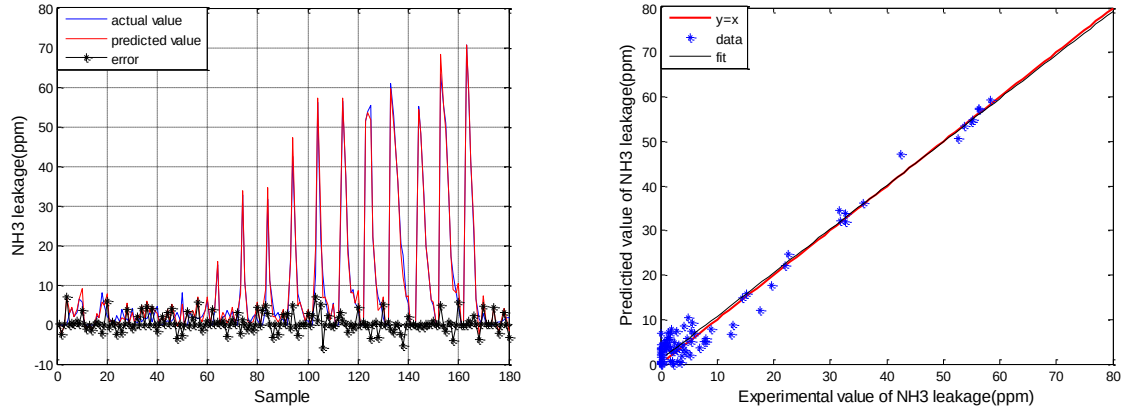

(a) (b)

Figure 7. Comparison between experimental and predicted values for NH_3 slip. (**a**) Actual *versus* predicted output; (**b**) Quality of fit.

The *RMSE* (root mean square error), *MAPE* (mean absolute percent error) and R^2 (correlation coefficient) values as well as the fits of the three models are given in Table 4.

Table 4. The fit statistics for the three prediction models.

Model	Upstream NO_x Emissions			Downstream NO_x Emissions			NH_3 Slip		
	Training	Test	All	Training	Test	All	Training	Test	All
RMSE(ppm)	24.62	57.16	44.01	19.56	25.87	21.87	1.34	2.84	2.22
MAPE(%)	1.71	4.77	3.24	2.17	6.89	4.53	-	-	-
R^2	0.99	0.98	0.99	0.99	0.98	0.99	0.99	0.97	0.98
Fits	Y1 = 0.9849 × X1 + 8.0395			Y2 = 0.9644 × X2 + 6.8769			Y3 = 0.9786 × X3 + 0.9270		

The *MAPE* for the upstream and downstream NO_x emission prediction models were under 5% for all datasets except for the test dataset for the downstream NO_x emissions, which were considered good enough for estimating the outputs. It was meaningless to calculate the *MAPE* for the NH_3 slip for the reason that the actual value of NH_3 slip may be 0 for certain particular working points, and the *MAPE* may not be defined mathematically (that is a constant divided by 0 cannot be defined mathematically). For example, it is difficult to achieve catalytic reduction when the temperature of SCR catalyst is under 200 °C. Under such a condition the urea injection amount is 0 and there is no NH_3 slip. The *RMSE* for three models of upstream NO_x emissions, downstream NO_x emissions and NH_3 slip were 44.01 × 10^{-6}, 21.87 × 10^{-6} and 2.22 × 10^{-6} respectively, which were considerably small, while the squared correlation coefficients for the three models were 0.99, 0.99 and 0.98 respectively. This implied that the accuracies of the three models were good enough for the prediction of the upstream and downstream NO_x emissions and NH_3 slip. The quality of fit between actual values and prediction values for the three models are also shown in Table 4.

It can be also seen from Table 4 that the *RMSE* and *MAPE* for the test datasets are a little larger than for the training datasets. The main reasons for this are as follows: Firstly, it was impossible to cover all the operating points of the diesel engine when choosing the training datasets for the model, which had a negative impact on the prediction accuracy. Secondly, some subjective factors existed in the parameter selection and data processing. Thirdly, there could be some outliers from such a large experimental data. Furthermore, there was no absolute guarantee that the experimental data would to be obtained in a completely steady state, and could lead to prediction errors as a consequence.

3.2. NSGA-II Multi-Objective Optimization Results

The prediction models for upstream NO_x emissions, downstream NO_x emissions and NH_3 slip are coded M1, M2 and M3, respectively, and are shown together with the inputs and outputs of the three models in Table 5.

Table 5. The inputs and outputs of the three prediction models.

Model	Inputs	Outputs
M1	Speed, Torque, Fuel supply pre cycle	Upstream NO_x emissions
M2	Temperature, Upstream NO_x emissions, urea injection amount	Downstream NO_x emissions
M3	Temperature, Upstream NO_x emissions, urea injection amount	NH_3 slip

Equations (5) and (6) were used as objective functions for the optimization framework using the NSGA-II genetic algorithm, with Equations (7) and (8) as inequality constraints. The aim of the current research was to maximize $Y\varepsilon$ (NO_x conversion efficiency) while minimizing the Y_{NH3} (NH_3 slip) using the NSGA-II genetic algorithm for the multi-objective optimization procedure discussed in Section 3.

$$Y\varepsilon = (M1 - M2)/M1 \quad (5)$$

$$Y_{NH3} = M3 \quad (6)$$

$$S.T\ M2 \geqslant 0 \tag{7}$$

$$M3 \geqslant 0 \tag{8}$$

where Y_{NH3} = the NH_3 slip (ppm); Yε = NO_x conversion efficiency (%); and M1, M2 and M3 represent the outputs of the three models, respectively.

To observe how the whole process functions, mode 4 in Table 3 was taken as an example, and the optimization was run and terminated after 200 iterations. Under certain operating speed, torque, fuel supply, temperature and upstream NO_x emissions were fixed. The only decision variable that could be changed by the researcher to deal with the trade-off between Yε (NO_x conversion efficiency) and Y_{NH3} (NH_3 slip) was the urea injection amount. Figure 8 shows the final 100 Pareto optimal solutions for the objective functions Yε (NO_x conversion efficiency) and Y_{NH3} (NH_3 slip), and their corresponding decision variables (urea injection amount) used for the multi-objective optimization. It could be seen from the graph that it is not possible to improve (increase) NO_x conversion efficiency without worsening (increasing) NH_3 slip. This trend generally characterizes a conflicting multi-objective optimization problem.

Among the 100 Pareto optimal solutions, in the initial stages there was a rapid increase in the NO_x conversion efficiency with the increase of the urea injection amount, while the value for NH_3 slip increased slightly. On the other hand, the NO_x conversion efficiency gradually decreased, while the rate of NH_3 slip gradually increased. Finally, NH_3 slip goes up rapidly with the increase of urea injection amount, while the NO_x conversion efficiency remains constant at 0.95.

For this particular multi-objective optimization problem, related emissions legislation (WHTC for Euro VI) requires that the real-time value of NH_3 slip should be less than 10 ppm. Therefore, a vertical line was drawn through the 10 ppm point on the horizontal axis, with the two points A(9.7, 0.88) and B(9.7, 940) which are closest to the left of vertical line (NH_3 slip less than 10 ppm) on the curves for the Pareto optimal frontier and the urea injection amount were taken as the optimal solution for the multi-objective problem under operating mode 4.

Point A represents the final optimal solution for the multi-objective optimization problem and point B is the corresponding urea injection amount under operating mode 4. In other words, for mode 4, with an upstream NO_x concentration of 684 ppm and a catalytic converter temperature of 250 °C, the optimal amount of urea which results in the optimal performance of the SCR catalytic converter (88% reduction of NO_x emissions and 9.7 ppm NH_3 slip) is 940 mL/h. Similar results for other working conditions can also be achieved using the same method. The optimization results for modes 4–9 (engine speed = 1500 rpm and 2000 rmp) of Table 3 are summarized and presented in Table 6. The designer can also obtain other optimal solutions to the multi-objective optimization problem from the Pareto front by setting other restrictions in the form of constraints.

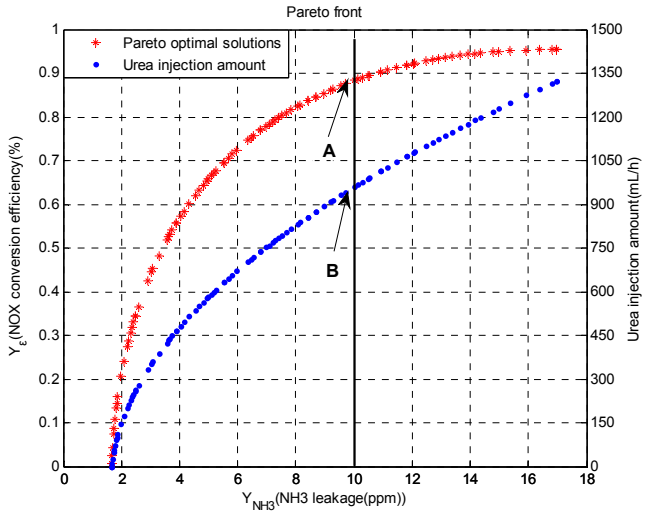

Figure 8. Pareto-based optimal solutions to the multi-objective optimization problem.

Table 6. Optimization results for the engine speeds of 1500 rpm and 2000 rpm.

Model	Speed (rpm)	Torque (N*m)	Temperature °C	Upstream NO_x (ppm)	Urea Injection Amount (mL/h)	NO_x Conversion Efficiency (%)	NH_3 Slip (ppm)
4	1500	204	250	684	940	88	9.7
5	1500	408	344	1131	1256	90	9.8
6	1500	612	415	1306	1553	90	9.6
7	2000	201	249	498	698	91	9.4
8	2000	395	318	767	1468	87	9.6
9	2000	596	394	1026	1178	92	9.3

4. Conclusions

A novel ensemble methodology with GA and SVM has been presented for establishing the models for the prediction of upstream and downstream NO_x emissions and the NH_3 slip. The various aspects of the modeling and optimization processes have been discussed in detail. The NSGA-II was used to solve the multi-objective optimization problem of maximizing NO_x conversion efficiency while minimizing NH_3 slip based on the decision variable of urea injection amount under certain operating points. Based on the current study, the following conclusions could be drawn:

(1) The prediction accuracy of the engine and SCR models could be improved by using an SVM, the parameters of which were optimized using a GA. The RMSE of upstream and downstream NO_x emissions and NH_3 slip for the all datasets was 44.01×10^{-6}, 21.87×10^{-6} and 2.22×10^{-6}, respectively. The MAPE of the models were all under 5%, and was good enough for estimating the actual outputs.

(2) The optimized urea injection amounts under certain operating points were obtained through multi-objective genetic algorithm for maximizing NO_x conversion efficiency while minimizing NH_3 slip.

Acknowledgments: The authors would like to express their deep appreciation to the Hubei Key Laboratory of Advanced Technology for Automotive Components (Wuhan University of Technology). The authors also wish to extend their appreciation to the National Natural Science Foundation of China (Grant No. 51406140) for financially supporting the study.

Author Contributions: All authors have contributed equally to the design of the research, data collection and analysis and the final preparation of the manuscript.

Conflicts of Interest: The authors declare no potential conflict of interest.

References

1. Brookshear, D.W.; Nguyen, K.; Toops, T.J.; Bunting, B.G.; Rohr, W.F. Impact of Biodiesel-Based Na on the Selective Catalytic Reduction of NO_x by NH_3 over Cu–Zeolite Catalysts. *Top. Catal.* **2013**, *56*, 62–67. [CrossRef]
2. Chen, P.; Wang, J. Nonlinear and adaptive control of NO/NO_2 ratio for improving selective catalytic reduction system performance. *J. Eng. Marit. Environ.* **2007**, *221*, 31–42. [CrossRef]
3. Iwasaki, M.; Shinjoh, H. A comparative study of "standard", "fast" and "NO_2" SCR reactions over Fe/zeolite catalyst. *Appl. Catal. A Gen.* **2010**, *390*, 71–77. [CrossRef]
4. Forzatti, P. Present status and perspectives in de-NO_x SCR catalysis. *Appl. Catal. A Gen.* **2001**, *222*, 221–236. [CrossRef]
5. Koebel, M.; Elsener, M.; Madia, G. *Recent Advances in the Development of Urea-SCR for Automotive Applications*; SAE International: Warrendale, PA, USA, 2001.
6. Majd, E.; Shamekhi, A.H. Development of a neural network model for selective catalytic reduction (SCR) catalytic converter and ammonia dosing optimization using multi objective genetic. *Chem. Eng. J.* **2010**, *165*, 508–516.
7. Beale, A.M.; Lezcano-Gonzalez, I.; Maunula, T.; Palgrave, R.G. Development and characterization of thermally stable supported V–W–TiO_2 catalysts for mobile NH_3–SCR applications. *Catal. Struct. React.* **2015**, *1*, 25–34. [CrossRef]

8. Karimi, H.R.; Zhang, H.; Zhang, X.; Wang, J.; Chadli, M. Control and Estimation of Electrified Vehicles. *J. Frankl. Inst.* **2015**, *352*, 421–424. [CrossRef]
9. Ardanese, R.; Ardanese, M.; Besch, M.C.; Adams, T.; Thiruvengadam, A.; Shade, B.C.; Gautam, M.; Oshinuga, A.; Miyasato, M. Development of an Open Loop Fuzzy Logic Urea Dosage Controller for Use with an SCR Equipped HDD Engine. In Proceedings of ASME 2009 Internal Combustion Engine Division Fall Technical Conference, Lucerne, Switzerland, 27–30 September 2009; pp. 353–363.
10. Hu, J.; Zhao, Y.; Zhang, Y.; Shuai, S. *Development of Closed-Loop Control Strategy for Urea-SCR Based on NO_x Sensors*; SAE Technical Paper; SAE International: Warrendale, PA, USA, 2011.
11. Willems, F.; Cloudt, R. Experimental demonstration of a new model-based SCR control strategy for cleaner heavy-duty diesel engines. *IEEE Trans. Control Syst. Technol.* **2011**, *19*, 1305–1313. [CrossRef]
12. Willems, F.; Cloudt, R.; van den Eijnden, E.; van Genderen, M. *Is Closed-Loop SCR Control Required to Meet Future Emission Targets?*; SAE International: Warrendale, PA, USA, 2007.
13. Herman, A.; Wu, M.; Cabush, D.; Shost, M. Model based control of SCR dosing and OBD strategies with feedback from NH_3 sensors. *SAE Int. J. Fuels Lubr.* **2009**, *2*, 375–385. [CrossRef]
14. Zambrano, D.; Tayamon, S.; Carlsson, B.; Wigren, T. Identification of a discrete-time nonlinear Hammerstein-Wiener model for a selective catalytic reduction system. In Proceedings of the American Control Conference (ACC), San Francisco, CA, USA, 29 June–1 July 2011.
15. Surenahalli, H.S.; Parker, G.; Johnson, J.H. *Extended Kalman Filter Estimator for NH_3 Storage, NO, NO_2 and NH_3 Estimation in a SCR*; SAE Technical Paper; SAE International: Warrendale, PA, USA, 2013.
16. D Ambrosio, S.; Finesso, R.; Fu, L.; Mittica, A.; Spessa, E. A control-oriented real-time semi-empirical model for the prediction of NO_x emissions in diesel engines. *Appl. Energy* **2014**, *130*, 265–279. [CrossRef]
17. Asprion, J.; Chinellato, O.; Guzzella, L. A fast and accurate physics-based model for the NO_x emissions of Diesel engines. *Appl. Energy* **2013**, *103*, 221–233. [CrossRef]
18. Maroteaux, F.; Saad, C. Combined mean value engine model and crank angle resolved in-cylinder modeling with NO_x emissions model for real-time Diesel engine simulations at high engine speed. *Energy* **2015**, *88*, 515–527. [CrossRef]
19. Lv, Y.; Yang, T.; Liu, J. An adaptive least squares support vector machine model with a novel update for NO_x emission prediction. *Chemom. Intell. Lab. Syst.* **2015**, *145*, 103–113. [CrossRef]
20. Taghavifar, H.; Mardanib, A.; Mohebbib, A.; Khalilaryaa, S.; Jafarmadara, S. Appraisal of artificial neural networks to the emission analysis and prediction of CO_2, soot, and NO_x of n-heptane fueled engine. *J. Clean. Prod.* **2016**, *112*, 1729–1739. [CrossRef]
21. Lv, Y.; Liu, J.; Yang, T.; Zeng, D. A novel least squares support vector machine ensemble model for NO_x emission prediction of a coal-fired boiler. *Energy* **2013**, *55*, 319–329. [CrossRef]
22. Vapnik, V.N.; Vapnik, V. *Statistical Learning Theory*; Wiley New York: New York, NY, USA, 1998; Volume 1.
23. Martínez-Morales, J.D.; Palacios-Hernández, E.R.; Velázquez-Carrillo, G.A. Modeling and multi-objective optimization of a gasoline engine using neural networks and evolutionary algorithms. *J. Zhejiang Univ. Sci. A* **2013**, *14*, 657–670. [CrossRef]
24. D Errico, G.; Cerri, T.; Pertusi, G. Multi-objective optimization of internal combustion engine by means of 1D fluid-dynamic models. *Appl. Energy* **2011**, *88*, 767–777. [CrossRef]
25. Shin, K.; Lee, T.S.; Kim, H. An application of support vector machines in bankruptcy prediction model. *Expert Syst. Appl.* **2005**, *28*, 127–135. [CrossRef]
26. Vapnik, V.N. The Nature of Statistical Learning Theory. *IEEE Trans. Neural Netw.* **1995**, *10*, 988–999. [CrossRef] [PubMed]
27. Severyn, A.; Moschitti, A. Large-Scale Support Vector Learning with Structural Kernels. *Lect. Notes Comput. Sci.* **2010**, *6323*, 229–244.
28. Tong, H.; Chen, D.R.; Yang, F. Learning Rates for -Regularized Kernel Classifiers. *J. Appl. Math.* **2013**, *2013*, 1–11. [CrossRef]
29. Dibike, Y.B.; Velickov, S.; Solomatine, D.; Abbott, M. Model Induction with Support Vector Machines: Introduction and Applications. *J. Comput. Civ. Eng.* **2001**, *15*, 208–216. [CrossRef]
30. Smola, A.J. Learning with kernels | Support Vector Machines. *Lect. Notes Comput. Sci.* **2008**, *42*, 1–28.
31. Goldberg, D.E. *Genetic Algorithms in Search Optimization and Machine Learning*; Addison-Wesley Professional: Boston, MA, USA, 1989; Volume 412.
32. Goldberg, D.E. *Genetic Algorithms*; Pearson Education: Upper Saddle River, NJ, USA, 2006.

33. Chen, R.; Sun, D.-Y.; Qin, D.-T.; Luo, Y.; Hu, F.-B. A novel engine identification model based on support vector machine and analysis of precision-influencing factors. *J. Cent. South Univ.: Sci. Technol.* **2010**, *41*, 1391–1397.
34. Zhou, H.; Zhao, J.P.; Zheng, L.G.; Wang, C.L.; Cen, K.F. Modeling NO_x emissions from coal-fired utility boilers using support vector regression with ant colony optimization. *Eng. Appl. Artif. Intell.* **2012**, *25*, 147–158. [CrossRef]
35. Deb, K. *Multi-Objective Optimization Using Evolutionary Algorithms*; John Wiley & Sons: New York, NY, USA, 2001; Volume 16.
36. Knowles, J.; Corne, D. The pareto archived evolution strategy: A new baseline algorithm for pareto multiobjective optimization. In Proceedings of the 1999 Congress on Evolutionary Computation, 1999, Washington, DC, USA, 6–9 July 1999.
37. Zitzler, E. *Evolutionary Algorithms for Multiobjective Optimization: Methods and Applications*; ETH Zurich: Zürich, Switzerland, 1999.
38. Coello, C.A.; Christiansen, A.D. Multiobjective optimization of trusses using genetic algorithms. *Comput. Struct.* **2000**, *75*, 647–660. [CrossRef]
39. Osyczka, A. Multicriteria optimization for engineering design. *Des. Opt.* **1985**, *1*, 193–227.